Arch. Metall. Mater. **67** (2022), 2, 601-606

DOI: https://doi.org/10.24425/amm.2022.137796

G. CALIN[1], L. SACHELARIE[1*], N. OLARU[2]

INFLUENCE OF SYNTHESIS CONDITIONS ON THE CHEMICAL STRUCTURE AND COMPOSITION OF ZnO NANOPARTICLES COMPOSITE SYSTEMS / POLYMER FIBERS

Nanostructured systems based on ZnO nanoparticles composite systems/polymer fibers have attracted a lot of attention in the last years because of their applications in multiple areas. Nanofibres based on polymers are used in many domains such as nanocatalysis, controlled release of medicines, environmental protection and so on. This work show the synthesis of cellulose acetate butyrate (CAB) nanofiber useful as substrates for growing ZnO nanocrystals and that ZnO is an unorganic metal oxide nanoparticle used to improve the piezoelectric properties of the polymer. The piezoelectric propertiesof ZnO-doped polymeric was investigated with atomic force microscopy and measurements were performed, in contact technique, in piezoelectric response mode (PFM).In order to analyze the structural and textural features, the obtained materials were characterized using advanced physical-chemical techniques such as X-ray diffraction (XRD), Atomic Force Microscopy (AFM), Scanning Electron Microscopy (SEM). The XRD patterns show the characteristic reflections of ZnO with a hexagonal type wurtzit structure and the broad peaks of the polymer. The SEM images reveal the presence of ZnO nanoparticles on top of the polymer nanofibres.In most ZnO-based nanocomposites their morphology is uncontrolled (agglomerated granules), but in ase of using cellulose acetobutyrate this becomes controlled by observing through flower-like structures SEM and AFM) The study of the functional properties of ZnO/polymer fiber composite systems showed that they have piezoelectric properties which give them the characteristics of smart material with possible sensor and actuator applications.Recent literature reports that the synthesis and characterization of ZnO-polymer nanocomposites are more flexible materials for various applications.

Keywords: polymer; nanofibres; composite ZnO/polimer; nanocomposites

1. Introduction

Due to their large surface area and porosity, nanofibers have various applications. The electrospinning process has proven to be a viable technique for producing nanofibers.The process of spinning fibers with the help of electrostatic forces is known as electrofilting. Recently it has been shown that the process of electrostatic spinning fiber is capable of producing fibers in the submicrometre [1]. In the literature, fibers with diameters less than 100 nm are generally called nanofibers [2]. These fibers, with smaller pores and larger surface area than ordinary fibers, have applications in nanocatalysis tissue engineering [3,4], controlled drug release protective clothing, security and defense, environmental engineering, filtering [5-7], power generation and optoelectronics [8-10].

The properties of a multifunctional polymer can be improved by using several nanoparticles [11,12]. Various metal oxides as nanoparticles are also widely used. ZnO is an unorganic metal oxide nanoparticle used to improve the properties of the polymer [8,13]. ZnO is an n-type metal oxide having a bandwidth of 3.37 eV; thus, it has excellent semiconductor properties. Recently, ZnO is widely used in optics, electronics, coating, elastomer, sunscreen and biomedical applications. Nanoscale coating of ZnO on suitable substrates is also important for potential applications for medical device. Medical devices from polymers, including the piezoelectric ones, are cheap in processing and material costs and most of the piezoelectric polymers become the right candidates for biomechanical devices, bioelectronics, and biological systems [13]. These medical devices can detect tissue deformations and give information about the mechanical properties of the skin surface. Opposite to the conventional equipment, these sensors can contact underlying topography with the skin surface [14].There are various ZnO synthesis methods that are available in many reports such as sol-gel method, hydrothermal synthesis, precipitation in water solution, precipitation from microemulsions, vapor deposition

[1] APOLLONIA UNIVERSITY OF IASI, FACULTY OF DENTAL MEDICINE, 11 PACURARI STR., 700511, IASI, ROMANIA
[2] INSTITUTE OF MACROMOLECULAR CHEMISTRY "PETRU PONI" IASI, ALEEA GRIGORE GHICA VODA,41A, 700487, IASI, ROMANIA

* Corresponding author: lisachero@yahoo.com

and mechanochemical processes [15]. The size and morphology of ZnO can be modified by regulating the synthesis conditions and reactants (Pholnak et al) regulated reaction time, temperature and mechanical forces during mixing of the reactants to synthesize ZnO [16,17]. They found that the morphology of ZnO changed with different temperatures. ZnO formed hexagonal prisms and hexagonal rods at 70 and 80°C, respectively [18]. The morphology changed from hexagonal rods to sword-like rods when they applied ultrasonic waves during the mixing of the reactants [15,19]. They also showed that the average particle size can be changed due to the concentration of reagents and that it also depends on the functional group attached [14].

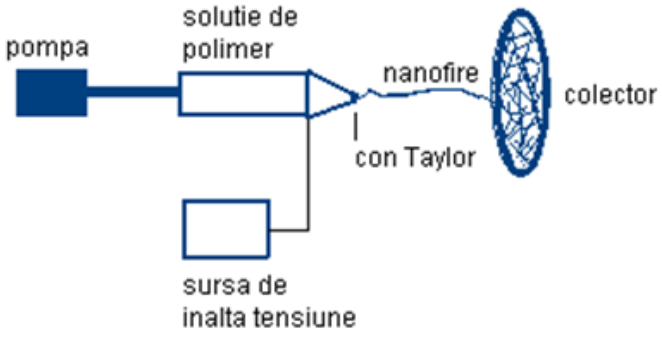

Fig. 1. Electrospinning installation

2. Methodology

Materials and methods

Using the method described in literature [12,14], a solution of ZnO nanoparticles was prepared as follows: 0.013 g of zinc acetate was dissolved in 4.8 ml of 2-methoxyethanol, then the solution was diluted to 55.2 ml with 2- methoxyethanol. The obtained solution was heated at 50°C, under magnetic stirring, for 1 hour. After clarifying the solution, it was cooled to 0°C and a solution of NaOH (0.0048 g in 4.8 ml of 2-methoxyethanol) was added dropwise. A specially constructed plant was used to obtain the cellulose acetobutyrate (CAB) nanofibers in the laboratory based on the principle of spinning in high voltage electric field ("electrospinning" procedure) Fig. 1. The process of electrophilating (spraying) in a high voltage field involves the formation of electrostatic charges in the mass of a polymer solution or melt in the presence of a high voltage electric field. Relaxation of the charges from the free surface of the fluid at the exit of the capillary leads to the formation of a so-called Taylor cone which produces a single jet of electrically charged fluid . It increases its speed and thins under the action of the electric field, finally being collected on a special metal surface. Relevant working parameters are fluid flow rate, electric field strength and current intensity between capillary and collector (20-40 □A). The flow rate (1-5 mL/h) is rigorously controlled by the pump, and the electric field, by the applied voltage (20 kV) or by the distance between the capillary and the collector (15 cm). The diameter of the formed fibers is affected by the applied electric field. Thus, the increase in voltage causes the increase in electrostatic forces which, in turn, causes the size of the nanofibers to decrease.

Cellulose acetobutyrate nanofibers are deposited in a thin, uniform layer, which easily detaches from the surface of the collecting disk. A solution of cellulose acetobutyrate (CAB) of 35% concentration (w/v) in a mixture of 2-methoxyethanol/DMF/2:1 (v/v) with a water content of 2% (vol.). Zinc acetate was added to the solution in a proportion of 17% relative to the polymer. The solution was electrophilated using a laboratory plant for high voltage field spinning. A uniform layer of zinc acetate nanofibers was obtained. Structural analyzes were performed by the X-ray diffraction (XRD) method, morphological analyzes by scanning electron microscopy (SEM) and piezoelectric properties by atomic force microscopy (AFM).

3. Result and discussion

The text continues here.The morphology of the ZnO/ polymer composite was investigated using scanning electron microscopy (SEM, VEGA II LSH). SEM micrographs show the presence of ZnO nanocrystals on CAB nanofibers (Fig. 2). The SEM images of ZnO/polymer nanocomposites obtained by a number of immersions in ammonium galvanizing solution show the presence of nanoparticles on the surface of nanofibers.

Nanocrystals are formed in the first immersion, their number and size being dependent on the number of immersions in the ammonium galvanizing solution.It is also observed that noparticles are present on both nanocomposites obtained by a number of 100 dives and those with 400 dives, so that this number seems to be less important beyond a certain value.

The characteristic diffractograms were obtained using the SHIMADZU 6000 diffractometer, with the following recording parameters: acceleration voltage, U = 40 kV, anodic current, I = 30 mA, the X-ray beam being monochromated with Å. The reflections were studied in the range of values (2θ = 0°-60°) (Fig. 3).

The structure of the samples was analyzed by identifying and indexing the diffraction peaks (maxima) in the characteristic X-ray diffractograms, according to the positions of the standard diffraction peaks and the corresponding Miller indices and the type of structure indicated in the ASTM (American Society for Testing Materials) published under the auspices of the JCPDS (Joint Committee for Powder Diffraction Standards).

In the interval 2θ = 30º-60º there are several peaks characteristic of zinc oxide, the most intense being (100), (002), (102), (110) and (101) respectively. The samples obtained are polycrystalline, with a hexagonal structure of wurtzite type.

The peaks belonging to cellulose acetobutyrate are very wide due to the polycrystalline structure which is not very well organized.The decrease in the solution concentration lowers to half or even to the disappearance of the peaks of zinc oxide. An increase in the number of immersions in the ammonium

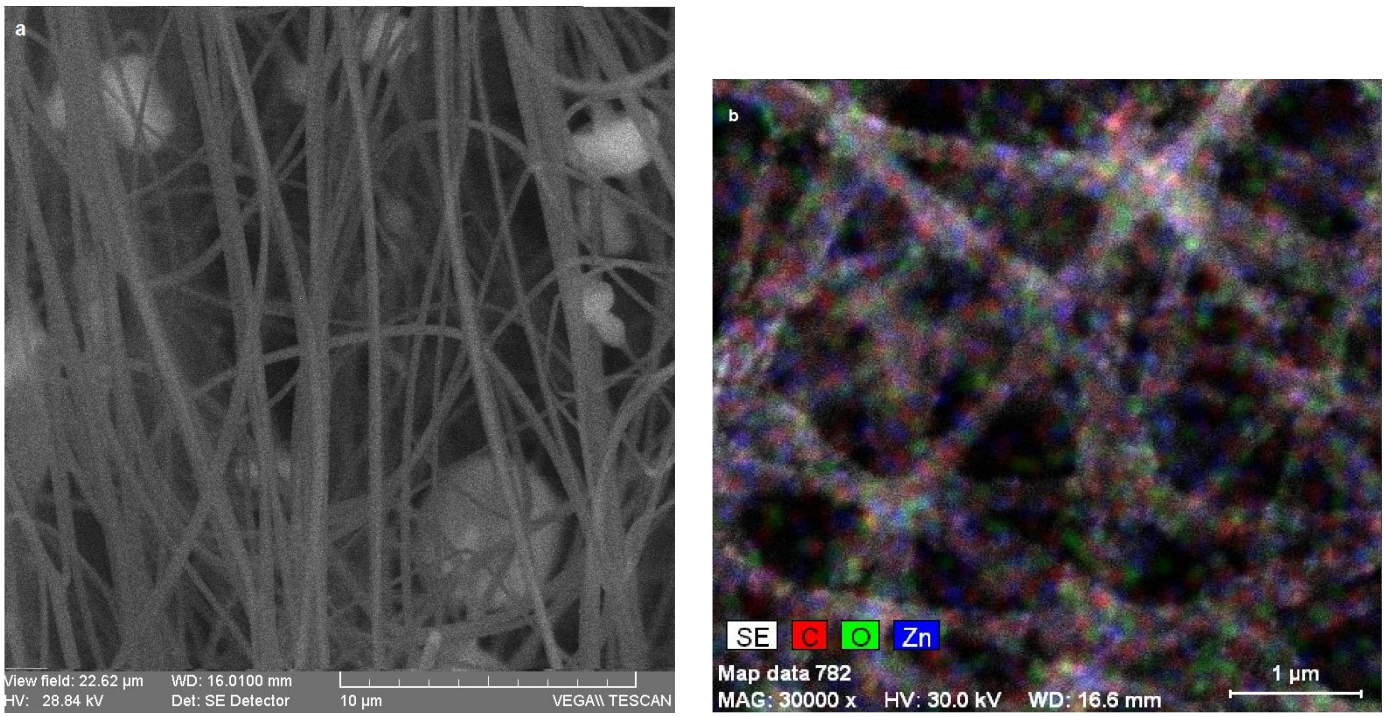

Fig. 2. SEM micrographs for: a) initial CAB nanofibers, without ZnO nanocrystals (image obtained before applying the immersion procedure); b) the ZnO/polymer composite obtained by performing a single immersion in the ammonium galvanizing bath.

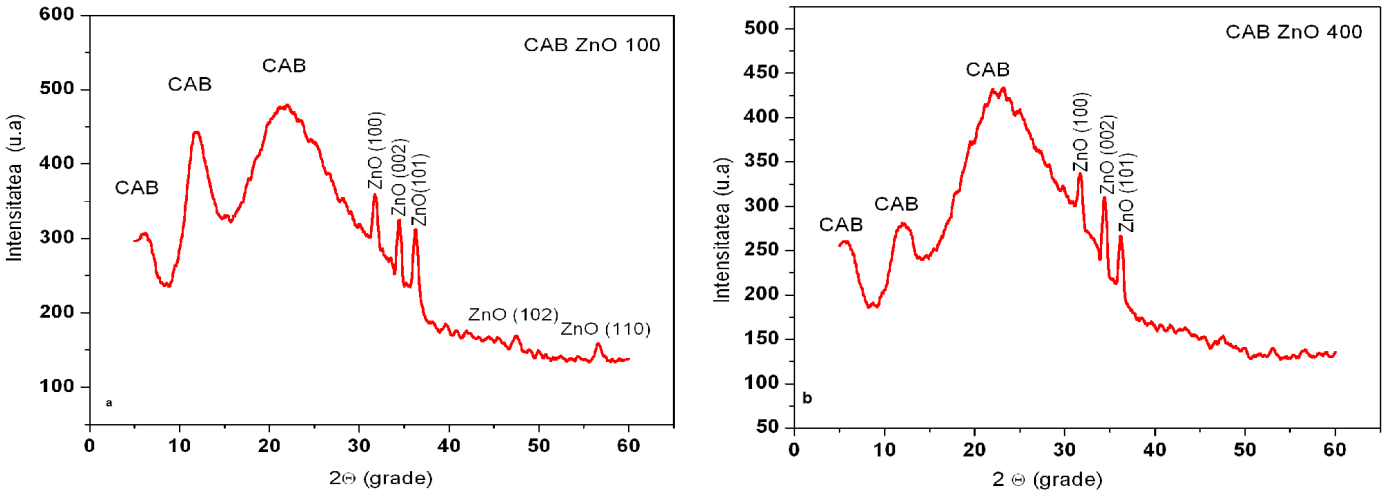

Fig. 3. X-ray diffractograms (CuKα) recorded for composite nanofibers: a) CAB ZnO 100, b) CAB ZnO 400

zincate solution causes a strong increase in the above-mentioned peaks from which we deduce that a large number of immersions causes a significant increase in the number of crystallites that are oriented parallel to the surface of the substrate with the plan (002).

To investigate the piezoelectric properties of ZnO-doped polymeric states, atomic force microscopy measurements were performed, in contact technique, in piezoelectric response mode (PFM), on a SolverPro NT-MDT system. Images obtained using the PFM technique were scanned at a frequency of 0.5 Hz, using platinum-coated conductive cantilevers with a peak radius of 10 nm, a free resonance frequency between 165 and 325 kHz, and a force constant between 0 .01 and 0.03 N/m. A voltage signal of the form VAC = V0 sin (ωt) with variable amplitude and frequency of 332 kHz was applied between the tip of the cantilever and the carbon band on which the samples were placed to record PFM images.

To obtain amplitude and phase images, the deflection signal from the cantilever is detected using the lock-in technique for which the following settings were used: Set Point = 2 nA, Feed-Back gain = 0.487, bandpass filter = 3 kHz. The amplitude of the first harmonic on the lock-in amplifier depends on the magnitude of the displacement and the phase change between the alternating electric field and the displacement of the cantilever. In this way, the magnitude of the displacement is recorded on one channel of the lock-in amplifier and the phase (orientation of the polar

domains) simultaneously on another channel. The magnitude signal represents the displacement (deformation) in the normal direction on the sample surface.

The phase signal provides information about the orientation of the domains, the upward-facing domains show positive contrast (they are bright in the phase images) and the downward-facing domains show negative contrast (they are dark in the phase images). This means that regions with opposite oriented polar domains will vibrate in phase opposition to each other when applying an alternating electric field and, therefore, appear as regions with strong contrast in the phase images (those without phase difference appear light in color and those with phase difference appear dark in color).

Thus, three samples were characterized by this method: a thin layer of zinc oxide deposited by sputtering, a layer of cellulose acetobutyrate (CAB) and a layer of cellulose acetobutyrate (CAB) immersed 25 times in zinc solution. of ammonium (Fig. 4).

The PFM tests performed on the cellulose acetobutyrate layer (CAB) are shown in Fig. 4, the topography images (a, d), magnitude (b, e) and phase (c, f) being obtained over a scanning area of 300×300 nm^2. Due to the flexibility of the polymer sample and the way it worked in contact, it was not possible to obtain clear topographic images on various scanning areas. In addition, when a low voltage (2V) was applied between the scanning tip of the cantilever and the carbon electrode on which the sample was placed, there was no change in the magnitude images (Fig. 5e) and phase (Fig. 5f), which indicates the absence of a piezoelectric response in the simple polymer.

Next, the same polymer was analyzed, this time immersed in a solution of ammonium galvanizing, 25 times, the topography images (a, d, g), magnitude (b, e, h) and phase (c, f , i) being obtained on a scanning area of 1×1 μm2. When no voltage signal was applied, the contrast in the magnitude (Fig. 5b) and phase (Fig. 5c) images was influenced only by the surface morphology shown in the topography image, this phenomenon being also called the edge effect. Before and after the application of a negative and a positive voltage signal, respectively, we notice in the magnitude images, a variation of the scale from –0.5 nA → 2 nA for B = 0 V (Fig. 5b) to –2 nA → 7 nA for B = –8V (figure 5e) and –10 nA → 15 nA for B = 8V (Fig. 5h), respectively, showing that the investigated sample shows a piezoelectric response. When applying a positive signal (B = 8 V), the fields that appear dark in the topography image (low areas) (Fig. 5g), are open in the magnitude (Fig. 5h) and the phase (Fig. 5i), which means that the crystallite vibrates in phase with the applied signal. When applying a negative signal (B = –8 V), the effect on these images is reversed (Fig. 5e, f).

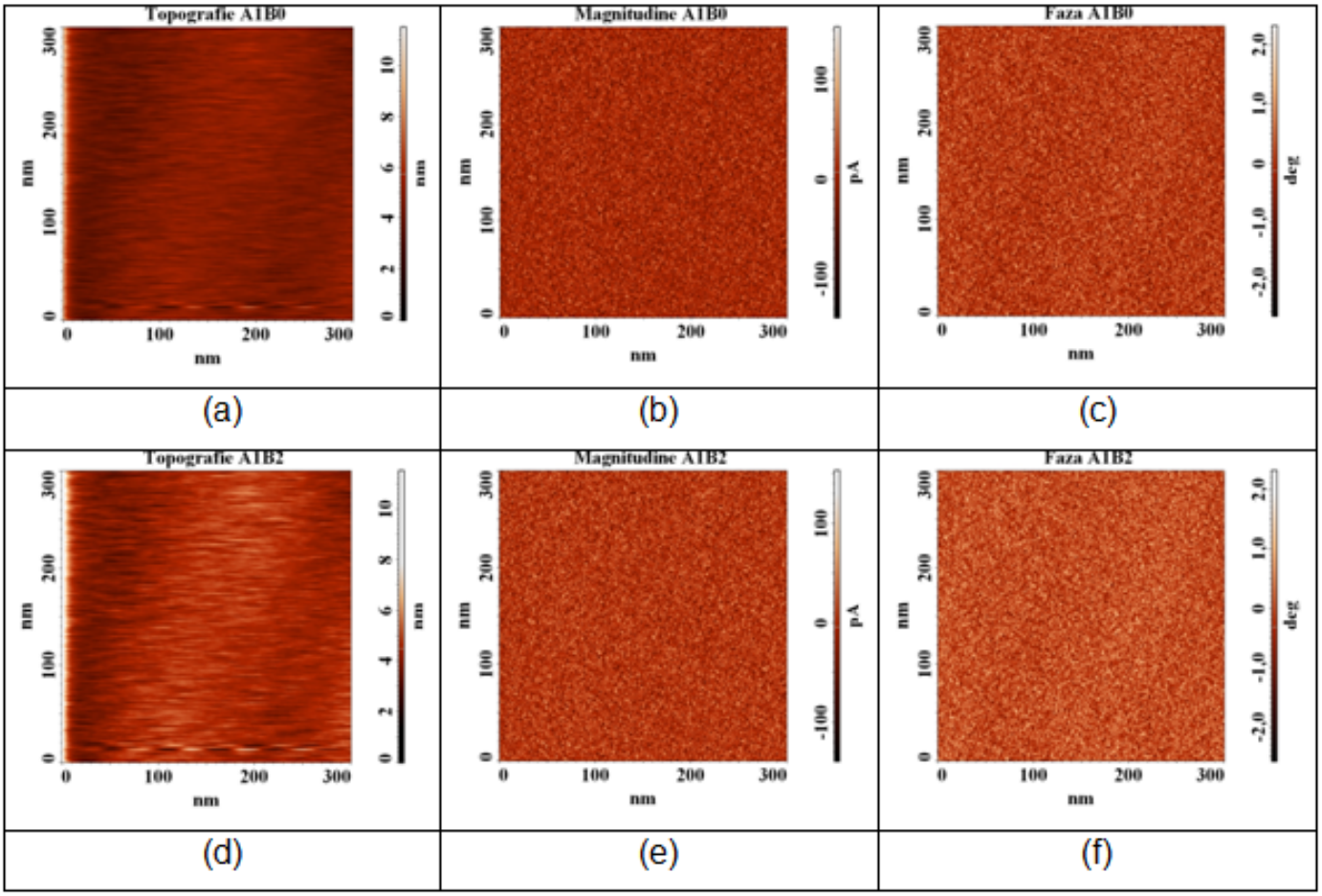

Fig. 4. Topography images (a, d), magnitude (b, e) and phase (c, f) obtained for the cellulose acetobutyrate layer (CAB) before (B = 0 V) and after the application of a voltage (B = 2 V)

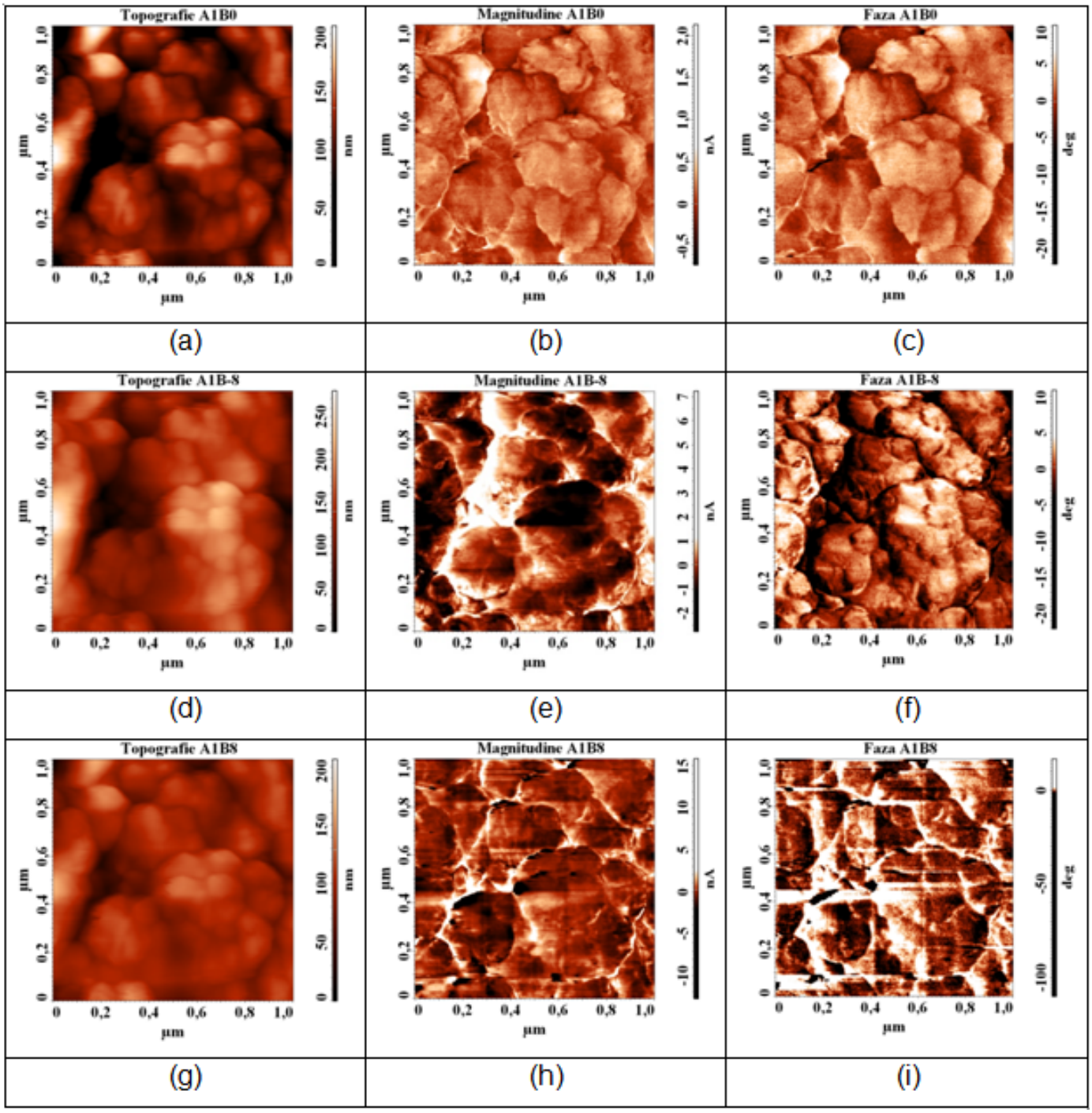

Fig. 5. Topography (a, d, g), magnitude (b, e, h) and phase (c, f, i) images obtained for the cellulose acetobutyrate (CAB) layer immersed 25 times in ammonium galvanizing solution, before (B = 0 V) and after applying a negative (B = –8 V) and positive (B = 8 V) voltage

4. Conclusion

This study indicate that SEM micrographs show the presence of ZnO nanocrystals on CAB nanofibers. These nanostructures occur regardless of the number of immersions in ammonium galvanizing. It is noticed that the particle size of ZnO does not depend on the number of immersions in the ammonium galvanizing bath. ZnO-based nanomaterials are a subject of increasing interest within current research, due to their multifunctional properties, such as piezoelectricity, semi-conductivity, as well as their low toxicity, biodegradability, low cost, and versatility in achieving various shapes. SEM studies have shown that ZnO nanocrystals develop on CAB nanofibers, regardless of the number of immersions in ammonium zincate; the particle size being independent of the number of dives. The application of the heat treatment determines the formation of well-defined ZnO nanoparticles, having a tendency to agglomerate. The synthesis conditions on the structure and chemical composition of ZnO/polymer composites are of a great importance in establishing its characteristics of being an smart material with various applications.

REFERENCES

[1] A. Król, P. Pomastowski, K. Rafińska, V. Railean-Plugaru, B. Buszewski, Zinc oxide nanoparticles: Synthesis, antiseptic activity and toxicity mechanism, Adv. Colloid. Interface. Sci. **249**, 37-52 (2017). DOI: https://doi.org/10.1016/j.cis.2017.07.033

[2] H. He, R. Chen, L. Zhang, T. Williams, X. Fang, W. Shen, Fabrication of single-crystalline gold nanowires on cellulose nanofibers, J. Colloid Interface Sci. **562**, 333-341 (2020). DOI: https://doi.org/10.1016/j.jcis.2019.11.093

[3] J. Ding, J. Zhang, Electrospun polymer biomaterials, Prog. Polym. Sci. **90**, 1-34 (2019). DOI: https://doi.org/10.1016/j.progpolymsci.2019.01.002

[4] D. Ponnamma, J.J. Cabibihan, Synthesis, optimization and applications of ZnO/polymer nanocomposites, Mater. Sci. Eng. C. **98**, 1210-1240 (2019). DOI: https://doi.org/10.1016/j.msec.2019.01.081

[5] D.M. Follmann, A.F. Naves, R.A. Araujo, O.N. Oliveira, Hybrid Materials and Nanocomposites as Multifunctional Biomaterials Curr. Pharm. Des. **23**, 3794-3813, (2017). DOI: https://doi.org/10.2174/1381612823666170710160615

[6] P. Pascariu, M. Homocianu, Preparation of La doped ZnO ceramic nanostructures by electrospinning-calcination method: Effect of La3+ doping on optical and photocatalytic properties, Appl. Surf. Sci. **476**, 16-27, (2019). DOI: https://doi.org/10.1016/j.apsusc.2019.01.077

[7] V. Anand, V.C. Srivastava, Zinc oxide nanoparticles synthesis by electrochemical method: Optimization of parameters for maximization of productivity and characterization, J. Alloys. Compd. **636**, 288-292, (2015). DOI: https://doi.org/10.1016/j.jallcom.2015.02.189

[8] J. Ding, J. Zhang, Electrospun polymer biomaterials, Prog. Polym. Sci. **90**, 1-34, (2019). DOI: https://doi.org/10.1016/j.progpolymsci.2019.01.002

[9] T. Blachowicz, A. Ehrmann, Most recent developments in electrospun magnetic nanofibers: A review, J. Eng. Fiber. Fabr. **15**, 1-6, (2020). DOI: https://doi.org/10.1177/1558925019900843

[10] M.Y. Song, D.K. Kim, K.J. Ihn, S.M. Jo, D.Y. Kim, Electrospun Nanofibers for Energy and Environmental Application, Synth. Met. **15** (1-3), 77-80, (2005).

[11] D.N. Phan, H.Y. Choi, S.-G. Oh, M. Kim, H. Lee, Fabrication of ZnO Nanoparticle-Decorated Nanofiber Mat with High Uniformity Protected by Constructing Tri-Layer Structure, Polymers. **12**, 1859, (2020). DOI: https://doi.org/10.3390/polym12091859

[12] C.M. Dumont, A.C. Mitchell, M.K. Munsell, J.C. Andrew, K. Strnadova, J. Park, B.J. Cummings, A.J. Anderson, L.D. Shea, Aligned hydrogel tubes guide regeneration following spinal cord injury, Biomaterials. **25** (5), 877-86, (2020). DOI: https://doi.org/10.1016/j.actbio.2018.12.052

[13] F. Yang, R. Murugan, S. Wang, S. Ramakrishna, Electrospinning of nano/micro scale poly(L-lactic acid) aligned fibers and their potential in neural tissue engineering, Biomaterials. **26** (15), 2603-10, (2005). DOI: https://doi.org/10.1016/j.biomaterials.2004.06.051

[14] D. Ponnamma, J.J. Cabibihan, M. Rajan, S.S. Pethaiah, K. Deshmukh, J.P Gogoi, S.K.K. Pasha, M.B. Ahamed, J. Krishnegowda, B.N. Chandrashekar, A.R. Polu, C. Cheng, Synthesis, optimization and applications of ZnO/polymer nanocomposites, Mater. Sci. Eng. C. **98**, 1210-1240, (2019). DOI: https://doi.org/10.1016/j.msec.2019.01.081

[15] M.S. Sorayani Bafqi, R. Bagherzadeh, M. Latifi, Fabrication of composite PVDF-ZnO nanofiber mats by electrospinning for energy scavenging application with enhanced efficiency, J. Polym. Res. **22**, 1-9, (2015). DOI: https://doi.org/10.1007/s10965-015-0765-8

[16] D. Shin, J. Kim, J. Chang, Experimental study on jet impact speed in near-field electrospinning for precise patterning of nanofiber, J. Manuf. Process. **36**, 231-7, (2018). DOI: https://doi.org/10.1016/j.jmapro.2018.10.011

[17] G. Prado-Prone, P. Silva-Bermudez, A. Almaguer-Flores, J.A. García-Macedo, V.I. García, S.E. Rodil, C. Ibarra, C. Velasquillo, Single-step, acid-based fabrication of homogeneous gelatinpolycaprolactone fibrillar scaffolds intended for skin tissue engineering, Int. J. Biol. Macromol. **14** (5), 1695-706, (2018). DOI: https://doi.org/10.1088/1748-605X/ab673b

[18] G. Hemamalini, V.R.G. Dev, Comprehensive review on electrospinning of starch polymer for biomedical applications, Int. J. Biol. Macromol. **106**, 712-8, (2018). DOI: https://doi.org/10.1016/j.ijbiomac.2017.08.079

[19] G. Liu, Z. Gu, Y. Hong, L. Cheng, C. Li, Electrospun starch nanofibers: Recent advances, challenges, and strategies for potential pharmaceutical applications, J. Control. Release. **28**, 252, 95-107, (2017). DOI: https://doi.org/10.1016/j.jconrel.2017.03.016